PLASTICS LABORATORY

TECHNICAL REPORT 13 B

* * * *

FERROMAGNETIC RESONANCE IN IRON OXIDES*

by

G. E. Crouch, Jr. and C. H. Willis

March 11, 1949

PRINCETON UNIVERSITY

P L A S T I C S L A B O R A T O R Y

T E C H N I C A L R E P O R T 13 B

* * * *

FERROMAGNETIC RESONANCE IN IRON OXIDES*

by

G. E. Crouch, Jr. and C. H. Willis

March 11, 1949

The research reported here was sponsored jointly by the Army; Signal Corps, and Navy Bureau of Ships, Bureau of Ordnance, Bureau of Aeronautics and Office of Naval Research under Signal Corps Contract No. W-36-039-sc-32011.

* A summary of this report appeared in the Physical Review, Vol. 75, 525, Feb. 15, 1949.

Ferromagnetic Resonance in Iron Oxides

by

G. E. Crouch, Jr. and C. H. Willis

* * * * *

Plastics Laboratory, Princeton University
Princeton, N. J.

Abstract

Natural ferromagnetic resonance in Fe_3O_4 and gamma-Fe_2O_3 is discussed, noting especially the broad region of resonance and a permeability appreciably less than unity. Values of the internal anisotropic magnetic field intensity for Fe_3O_4 and gamma-Fe_2O_3 are calculated. It is shown that the absorption mechanism cannot be represented by an idealized damped oscillator or Gaussian absorption mechanism. An explanation of the observed ferromagnetic resonance is offered.

* * * * * *

I. Introduction

Magnetic resonance occurs when the frequency of an alternating magnetic field corresponds with the precession frequency of a magnetic dipole about a central magnetic field. The frequency at which resonance occurs depends upon the strength of the central magnetic field and, in general, occurs in the microwave region for ferromagnetic resonance or electron spin precession, and in the radio frequency region for paramagnetic resonance or nuclear spin precession. Natural magnetic resonance occurs when the central magnetic field about which there is precession is due to the natural internal field of the material, as distinguished from induced magnetic resonance caused by a static externally applied field.

Permeability versus frequency relations involving resonance are somewhat similar in appearance to dispersion in metallic powders although due to a different phenomenon. In the latter the skin depth decreases with increase in frequency so that an applied alternating magnetic field penetrates only a certain distance below a surface boundary. The resulting magnetization correspondingly decreases and a decrease in permeability is observed with increase in frequency.

Natural ferromagnetic resonance has been observed only recently, by Birks[1]. This is understandable because, first one must investigate a ferromagnetic material that has a sufficiently low electrical conductivity so that the alternating magnetic field can penetrate the material, and secondly,

---

[1] J. B. Birks, Nature, 160, 535 (1947)

due to the internal magnetic field intensity the resonant frequency lies in the microwave region which has only recently become available for investigation.

It is interesting that Landau and Lifschitz[2] first predicted such a resonance from a classical analysis of ferromagnetic domains. However demagnetizing fields, eddy current damping, and magneto strain were not considered. It has, however, been shown that eddy current losses do not introduce damping terms in the permeability. The induced resonant frequency is affected by demagnetizing fields and specimen shapes as well as crystalline anisotropy energy[3].

A detailed quantum mechanical analysis of ferromagnetic resonance so as to predict the absorption band shape theoretically has not been reported. It has been pointed out by Van Vleck[4] that in the case of paramagnetic resonance such an analysis is prohibitively difficult. The analysis of ferromagnetic resonance seems to be no less difficult. Some idea of the line width in paramagnetic resonance is obtained, however, from the second moment of the frequency deviation. Line widths found in the latter case are in the neighborhood of several hundred kilocycles, whereas in ferromagnetic resonance the absorption may extend over several thousand megacycles.

An attempt to explain the band width from a simple analysis will be

---

2 Landau and Lifschitz, Physik. Zeits. Sowjetunion 8, 153 (1935)

3 C. Kittel, Phys. Rev. 73, 155 (1948)

4 J. H. Van Vleck, Phys. Rev. 74, 1168 (1948)

presented. It will be seen that this analysis indicates band widths which agree in order of magnitude with those observed. The simplification presented seems somewhat justified in view of the success of a similar interpretation of nuclear resonance absorption and because a more rigorous analysis[5] for nuclear absorptions yields results substantially in agreement with those obtained from the simpler calculations.

II. Examination of the observed Permeability versus Frequency curves of Fe_3O_4 and gamma-Fe_2O_3

Curves of the magnetic permeability, ($\mu' - j\mu''$) of Fe_3O_4 powder and gamma-Fe_2O_3 powder are shown in Fig. 1 and Fig. 2. Permeabilities are extrapolated to 100% concentration with Lichtenecker's relation. These curves are drawn from composite data which Birks[1] has given and which we have obtained at 1.2 cm. It is interesting to note that the permeability, μ', becomes appreciably less than unity at certain frequencies and that there is a broad region of natural ferromagnetic resonance. This resonance has been interpreted as being due to the interaction of a magnetic field at microwave frequencies with the Larmor spin precession about the internal anisotropic magnetic field. The resonance frequency is given by

$$\nu_m = \frac{g\mu_e}{h} H_m$$

μ_e is the magnetic moment of the electron in Bohr magnetons, H_m is the internal field intensity in Gauss, h is Planck's constant, and g is the Lande factor which is 2 for electron spins. For each value of ν_m there

---

[5] G. E. Pake, J. of Chem. Phys. 16, 327, (1948)

is a corresponding value of $1/\mu$ so that the curves in Fig. 1 and Fig. 2 may be thought of in terms of a spectrum of values of $1/\mu$ about which there is spin precession.

Examination of the permeability curves with regard to the Kronig-Kramers[6] susceptibility relations -

$$\chi'(\nu) - \chi'(\infty) = \frac{2}{\pi} \int_0^\infty \frac{\nu' \chi''(\nu')}{\nu'^2 - \nu^2} d\nu'$$

$$\chi''(\nu) = -\frac{2\nu}{\pi} \int_0^\infty \frac{\chi'(\nu) - \chi'(\infty)}{\nu'^2 - \nu^2} d\nu$$

indicates that, by comparing various calculated curves to the observed curves, one can more nearly approximate conditions with a damped oscillator absorption curve than with a Gaussian absorption curve. The frequency dependence of $\chi''(\nu)$ is given by -

$$\chi''(\nu) = \pi \chi_0 \nu_m g_m(\nu)$$

$$\int_0^\infty g(\nu) d\nu = 1 \quad , \quad T_2 = \frac{1}{2} \left[g(\nu) \right]^{1/2}_{max.}$$

χ_0 being the static ferromagnetic susceptibility.

Since both of these shape functions may be linked with idealized physical models, some insight into the absorption mechanism may be gained, although considering the experimental accuracy of measuring μ'' there is doubt as to whether this is feasible. If the damped oscillator idea is pursued, it is necessary to consider the local field variations at Larmor frequencies due to neighbors which affect a given dipole. The Gaussian idea of a variation of static local fields to change the resonant values of

---

[6] G. E. Pake and E. M. Purcell, Phys. Rev. 74, 1184, (1948)

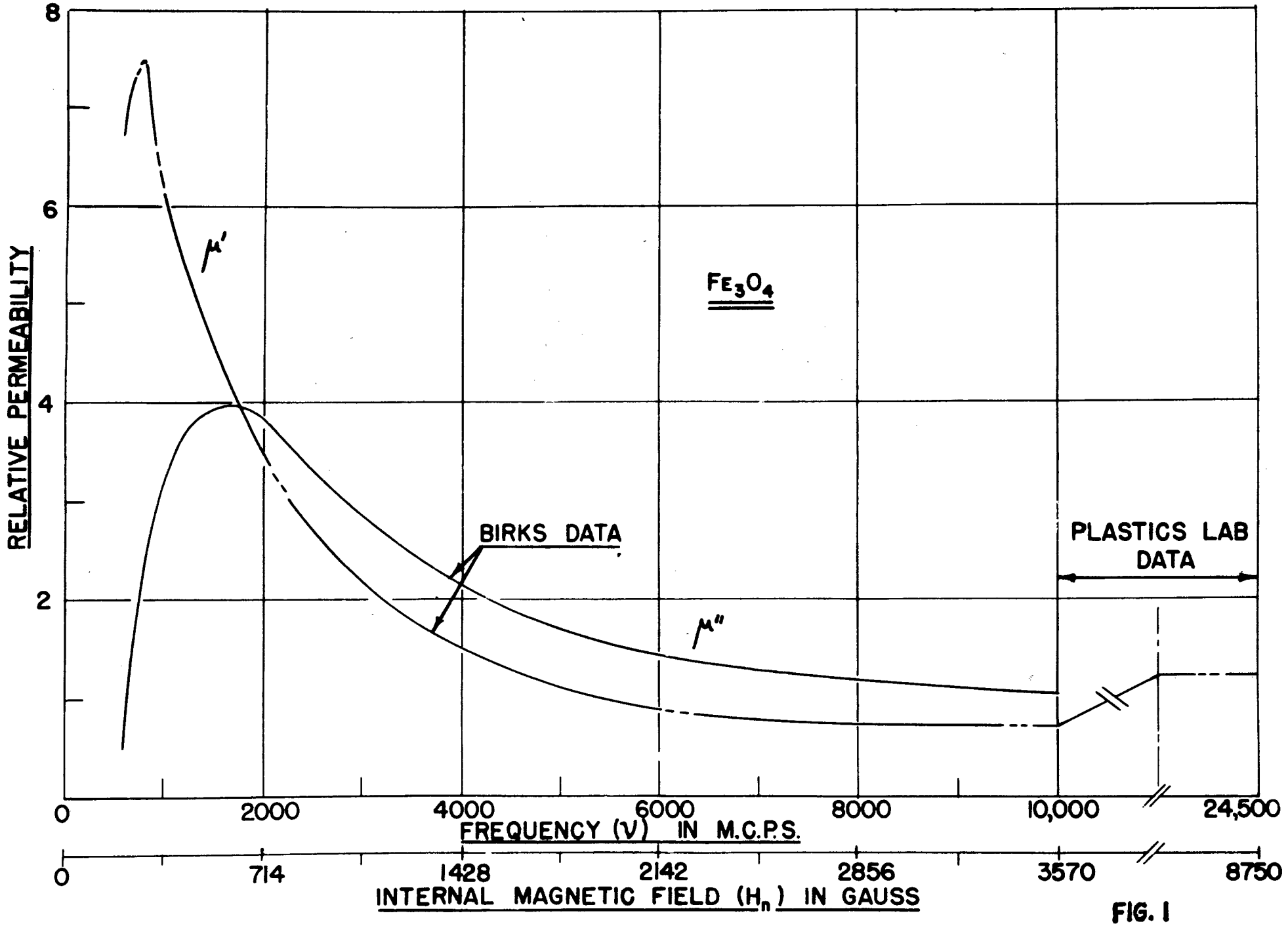
8
6
4
2
RELATIVE PERMEABILITY
μ'
μ''
Fe3O4
BIRKS DATA
PLASTICS LAB DATA
0
2000
4000
6000
8000
10,000
24,500
FREQUENCY (ν) IN M.C.P.S.
0
714
1428
2142
2856
3570
8750
INTERNAL MAGNETIC FIELD (Hn) IN GAUSS

FIG. 1

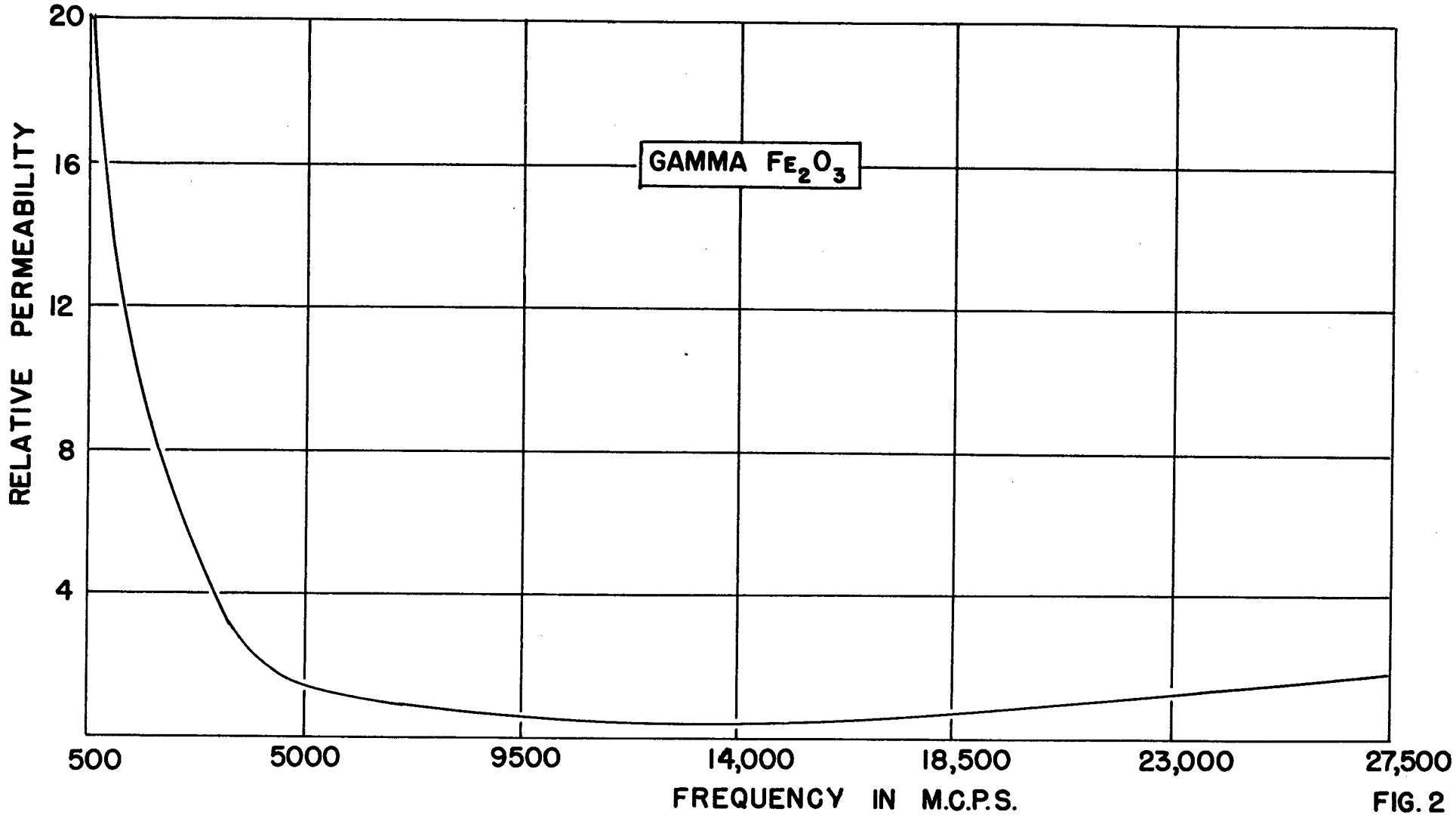
20
16
12
8
4
RELATIVE PERMEABILITY
GAMMA Fe_2O_3
500
5000
9500
14,000
18,500
23,000
27,500
FREQUENCY IN M.C.P.S.

FIG. 2

the constant magnetic field seems to be simpler to apply even though not in agreement with a damped oscillator idea. Further discussion of this Gaussian distribution of spins to produce a continuously varying local magnetic field will be given in section III.

There remains a considerable discrepancy between the expected μ' curve and the observed μ' curve, the latter being more reliable than the observed μ'' curve. This is seen by referring to Figs. 3,4 and 5. These curves are plotted from the following relations –

$$\chi''(\omega) = \chi_0 \omega_0 T_2 \frac{1}{1 + T_2^2(\omega_0 - \omega)^2}$$

$$\chi'(\omega) = \chi_0 \omega_0 T_2 \frac{T_2(\omega_0 - \omega)}{1 + T_2^2(\omega_0 - \omega)^2}$$

$$\frac{\omega_0}{2\pi} = \nu_0 = \text{resonant frequency}$$

which are in accord with the Kronig-Kramers relations. The parameters to be varied in order to fit the observed curves are T_2, ω_0 and χ_0. $\chi_0 \omega_0 T_2$ is taken as 4. T_2 is calculated from the shape function $g(\nu)$ and is found to be $\frac{1}{17,500}$ sec. for a damped oscillator and $\frac{1}{8320}$ sec. for a Gaussian shape function. The curves in Fig. 3 are plotted for the damped oscillator with $\omega_0 = 9420$ mrps; Fig. 4 for a damped oscillator and $\omega_0 = 32,600$ mrps; Fig. 5 for a Gaussian distribution and $\omega_0 = 9420$ mrps. Fig. 4 was plotted because it had been previously suggested that, in order to obtain a g factor of 2, Hn was such that $\omega_0 = 32,600$ mrps. It is rather obvious from the lack of agreement of the curves of Fig. 4 and Fig. 1 that this does not explain the discrepancy. In all cases μ' increases at the higher frequencies to larger values than those observed so that obviously other considerations to explain shape functions different from the two idealizations chosen here are necessary. In all cases there is considerable discrepancy between the experimental and the calculated curves. However,

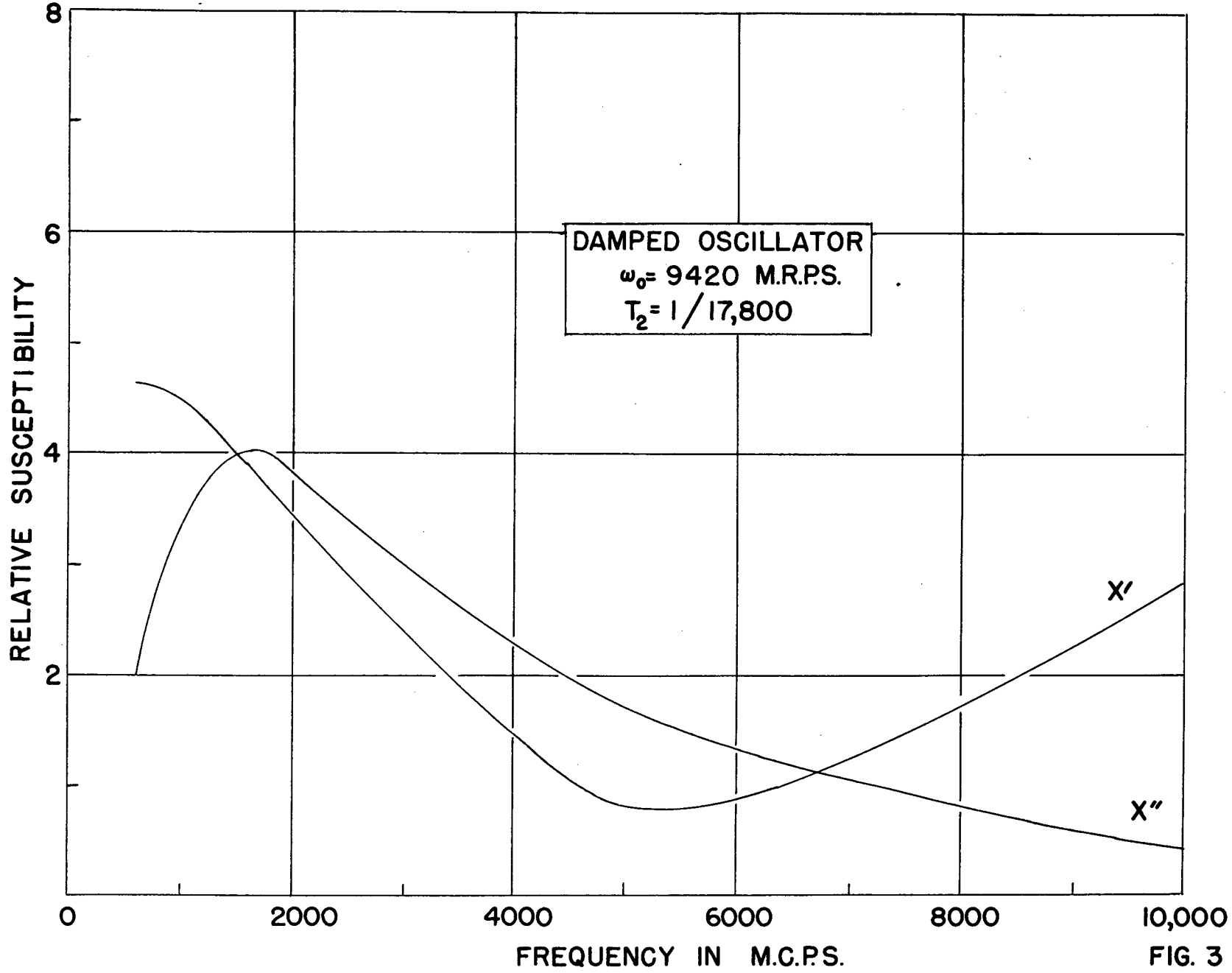
DAMPED OSCILLATOR
ω_0= 9420 M.R.P.S.
T_2= 1/17,800
RELATIVE SUSCEPTIBILITY
8
6
4
2
0
2000
4000
6000
8000
10,000
FREQUENCY IN M.C.P.S.
X′
X″

FIG. 3

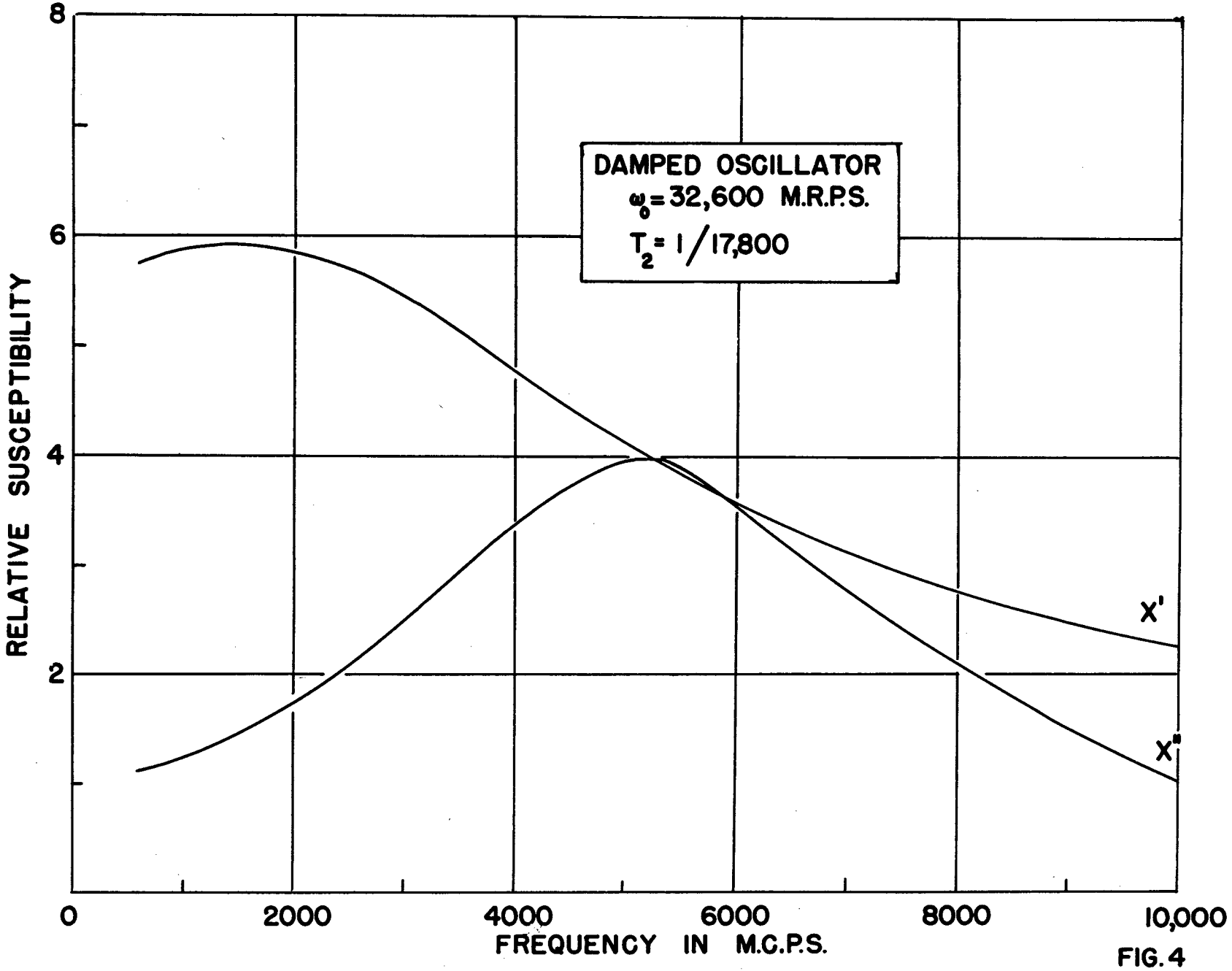
DAMPED OSCILLATOR
ω_0 = 32,600 M.R.P.S.
T_2 = 1/17,800
X'
X''
RELATIVE SUSCEPTIBILITY
8
6
4
2
0
2000
4000
6000
8000
10,000
FREQUENCY IN M.C.P.S.

FIG. 4

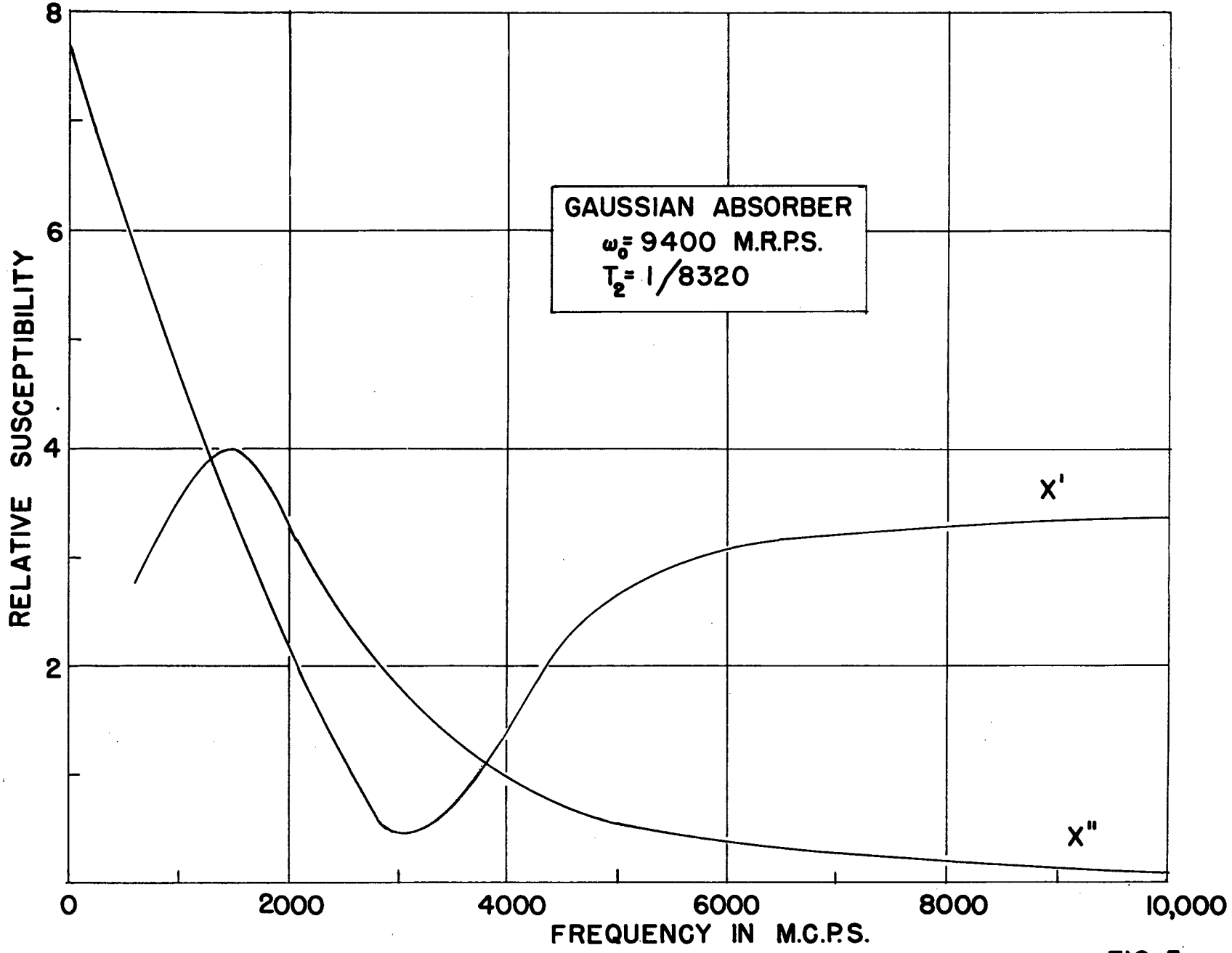
GAUSSIAN ABSORBER
ω_0= 9400 M.R.P.S.
T_2= 1/8320
X'
X"
RELATIVE SUSCEPTIBILITY
8
6
4
2
0
2000
4000
6000
8000
10,000
FREQUENCY IN M.C.P.S.

FIG. 5

reasonable values of H_m and ν_m seem to be

$$H_m \cong 600 \text{ Gauss}$$
$$\nu_m \cong 1700 \text{ mcps}$$

For the second moment of the shape function as defined by Van Vleck[4]

$$\langle (\Delta\nu)^2 \rangle_{ave}^{1/2} \cong \int_0^\infty g(\nu) \Delta\nu^2 \, d\nu$$

It is found that

$$\left[(\Delta\nu)^2 \right]^{1/2} \cong 1300 \text{ mcps}$$

In conclusion then, it appears that an idealized mechanism such as a Gaussian or damped oscillator does not represent the resonant mechanism for Fe_3O_4 and gamma-Fe_2O_3. Reasonable values of the internal anisotropic magnetic fields appear to be

$$H_m \cong 600 \text{ Gauss for } Fe_3O_4$$
$$H_m \cong 400 \text{ Gauss for gamma-}Fe_2O_3$$

In the discussion of the permeability curves we have been concerned primarily with Fe_3O_4 rather than gamma-Fe_2O_3 because a more complete curve for Fe_3O_4 is given; that is, both peaks of the resonance curve are seen. Also Fe_3O_4 crystallizes in the cubic system whereas gamma-Fe_2O_3 crystallizes in the hexagonal system. The general considerations seem to be parallel for the two materials with the curves for gamma-Fe_2O_3 displaced toward lower frequencies. This indicates a smaller value of the internal magnetic field, a fact which is not inconsistent with the crystalline structure of the materials and the larger separation of the iron atoms.

III. A Proposed Ferromagnetic Resonance Explanation

A possible explanation of the observed broad ferromagnetic resonance absorption seems to lie in the interaction of magnetic dipoles to perturb

the value of the internal magnetic field about which there is spin precession. Each iron atom is represented by an atomic dipole with a magnetic moment, μ_a. These dipoles are situated at definite positions in the cubic Fe_3O_4 lattice. Each dipole is in an effective magnetic field due to a constant internal field and a fluctuating magnetic field produced by its neighbors. That is,

$$H_{eff} = H_m \pm \frac{a\mu_a}{a^3}$$

where a is a parameter that will be of the order of magnitude of 1 or 2 and a is the distance between neighboring dipoles. Here we have made the assumption that all dipoles are pointing either in the same direction or the opposite direction to the internal field. It can be seen that a is related to the space distribution of dipoles and that a consideration of all dipoles surrounding a given dipole would tend to give a continuous variation of values of H_{eff} somewhat as shown in Fig. 6.

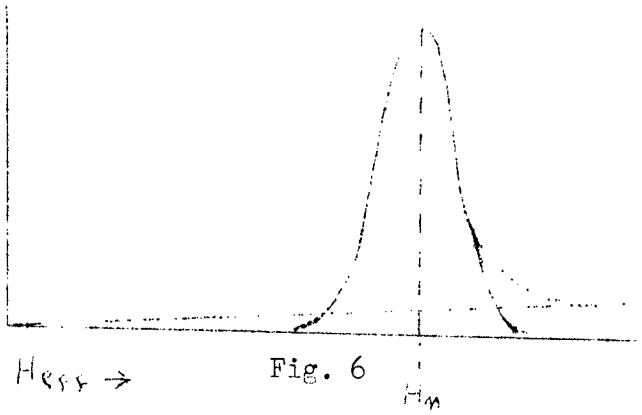

Fig. 6

Here a Gaussian distribution, as previously discussed, is shown. This is justifiable if one is able to assume a randomness of distribution of dipole directions for the neighbors of a given dipole, an assumption, which as previously stated, does not seem to be completely justified by the observations. Nevertheless, one would be led to expect the width ($\Delta\nu$) of the

absorption band to be of the order of magnitude of $\mu_z/2\sqrt{3}$. On this basis, the calculated values of ΔH and $\Delta \nu$ are:

$$\Delta H \cong 1400 \text{ Gauss}$$

$$\Delta \nu \cong 5000 \text{ mcps}$$

These calculated values can be seen from Fig. 1 to be rather consistent with observations. In calculating ΔH, μ_z has been taken as 2 Bohr magnetons, R has been taken as 3 A°. and α has been taken as 1. The omission of certain factors in this simplification seems somewhat justified because a more rigorous analysis in the case of nuclear absorption gives results substantiating the simpler assumptions. Also, it would appear that factors entering a more rigorous analysis would perhaps be difficult to examine because of experimental accuracy in measuring μ' and μ''.

IV. Permeability Measurements

Permeability measurements in the microwave region were made following a method which has been previously described in the Princeton University Plastics Report No. 10, page 828, and will therefore not be repeated here. Suffice it to say that permeabilities were calculated from the following expressions:

$$Z_g = (\mu' - j\mu'') \frac{\gamma_g}{\gamma_\ell}$$

The quantities measured were Z_g, the per unit characteristic impedance of the powder filled wave guide, γ_g, the propagation constant along the air-filled wave guide, and γ_ℓ, the propagation constant along the powder filled wave guide.

An analysis of sources of error has been given previously in the Plastics

Laboratory Report No. 9, page 738. By the method employed here it is thought that μ' is measured to an accuracy of 10% and μ'' is measured to an accuracy of 20%.

V. Conclusions

In an extension of the investigation reported here several interesting ideas suggest themselves as possibilities for future consideration. From an analysis of the absorption curve it is seen that $\Delta H = \frac{2a\mu_0}{r^3}$ This offers, therefore, a means of calculating r, the separation of the iron atoms in the iron oxide compound. However, the accuracy of determining r from x-ray measurement is greater than one could achieve here. (It should be remarked in passing that a similar analysis of the absorption line for nuclear resonance enables a calculation of the proton-proton distance[6] in certain compounds where an x-ray analysis fails to locate the protons.) Perhaps the most interesting possibility, since r has been measured quite accurately by x-ray methods, is a calculation of the magnetic moment of the un-ionized iron atom.

In extending the analysis to measure these quantities an improvement in the experimental accuracy is desirable as well as a more rigorous analysis to indicate more precisely the parameter a. This would involve some considerations of geometric arrays of dipoles. Magnetic field intensities at various positions in a cubic array of dipoles have been calculated by McKeehan[7] but in that analysis all dipoles have been considered to point in the same direction.

In the case of Fe_3O_4 the resonant frequency is related to the quantity $\frac{K_1}{M_s}$ as shown by Kittel[3]. Here K_1 is the first order cubic anisotropic energy constant and M_s is the saturation magnetization. This therefore offers an evaluation of the anisotropic energy.

---

[7] L. W. McKeehan, Phys. Rev. 43, 913, (1933).

Revised Distribution List for Technical and Final Reports Issued
by Princeton University Joint Service Contract W36-039-sc-32011

Office of the Chief Signal Officer
Engineering & Technical Division
National Defense Bldg.
Washington 25, D. C. (2 cys)

Signal Corps Liaison Engineer
Engineer Research & Development Labs.
Fort Belvoir, Va. (1 cy)

Engineer Research & Development Div.
Office of the Chief of Engineers
Gravelly Point, Va. (1 cy)

Office of the Chief of Ordnance
Washington 25, D. C. (1 cy)

Signal Corps Liaison Engineer
Office, Chief of Ordnance
Detroit Arsenal
Centerline, Michigan (1 cy)

Signal Corps Liaison Officer
Mass. Institute of Technology
Cambridge, Mass. (1 cy)

Army Liaison Officer, Code 140
U. S. Navy Electronics Lab.
San Diego 52, Calif. (1 cy)

Commanding General
Air Materiel Command
Wright Field
Dayton, Ohio (4 cys)

Commanding Officer
Watson Labs, AMC
Red Bank, N. J. (2 cys)

Commanding Officer
Cambridge Field Station
230 Albany Street
Cambridge, Mass. (1 cy)

Director
National Bureau of Standards
Washington, D. C. (1 cy)

Chairman, Research & Development Board
National Defense Bldg.
Washington 25, D. C. (1 cy)

Armour Research Foundation of the
Illinois Inst. of Technology
Chicago, Ill. (ATTN: E. Nielson)
(1 cy)

Federal Telecommunications Lab, Inc.
500 Washington Ave.
Nutley, N. J. (ATTN: F. A. Muller)(1cy)

Interchemical Corporation
432 W. 45th Street
New York, N. Y. (ATTN: Dr. L.J. Radi
1 cy and Dr. A.G. Chenicek 1 cy)

Polaroid Corporation
730 Main Street
Cambridge, Mass. (ATTN: Dr. E.R. Blout)
(1 cy)

Vita-Var Corporation
Raymond Commerce Bldg.
Newark, N. J. (ATTN: Mr. A. O. Allen)
(1 cy)

Rutgers University
New Brunswick, N. J.
(ATTN: Dr. John Koenig) (1 cy)

Brooklyn Polytech. Institute
99 Livingston Street
Brooklyn, N. Y. (1 cy)

Transportation Officer
Signal Corps Engineering Laboratories
Evans Signal Laboratory
Bldg. 42, Belmar, N. J.
MARKED: For Signal Property Officer
File No. 13901-PH-48-91(6465)
(16 cys)

Current Members of the ASTM Advisory
Committee (1 cy each)

Chief of Naval Research
Department of Navy
Washington 25, D. C.
ATTN: Code 423 (11 cys)

Chief of Naval Research
Department of Navy
Washington 25, D. C.
ATTN: Code 425 (1 cy)

Commanding Officer
New York Branch Office
Office of Naval Research
Building 3, 10th Floor
N. Y. Naval Shipyard
Brooklyn 1, N. Y. (2 cys)

Commanding Officer
Chicago Branch Office
Office of Naval Research
844 N. Rush Street
Chicago 11, Illinois (1 cy)

Commanding Officer
San Francisco Branch Office
Office of Naval Research
801 Donahue Street
San Francisco, Calif. (1 cy)

Commanding Officer
Boston Branch Office
Office of Naval Research
495 Summer Street
Boston 10, Mass. (1 cy)

Solid Propellant Information Agency
Johns Hopkins University
Applied Physics Laboratory
Silver Spring, Md. (2 cys)

Commanding Officer
Picatinny Arsenal
Dover, New Jersey
ATTN: Dr. L. Gilman (1 cy)

Commanding Officer
Naval Ordnance Test Station
Inyokern, Calif.
ATTN: Dr. J. H. Wiegand (1 cy)

Commanding Officer
Los Angeles Branch Office
Office of Naval Research
1030 E. Green Street
Pasadena, Calif. (1 cy)

Director, Naval Research Laboratory
Department of Navy
Washington 20, D. C. (2 cys)

Ass't. Naval Attache for Research
Naval Attache
American Embassy
Navy #100
c/o Fleet Post Office
New York, N. Y. (5 cys)

Chief, Bureau of Ordnance
Department of Navy
Washington 25, D. C.
ATTN: Code Re1 (1 cy)

Chief, Bureau of Ordnance
Department of Navy
Washington 25, D. C.
ATTN: Code Re2d (1 cy)

Chief, Bureau of Ordnance
Department of Navy
Washington 25, D. C.
ATTN: Code Ad3 (3 cys)

Commanding Officer
Naval Powder Factory
Indian Head, Md.
ATTN: Dr. W. J. Moore (1 cy)

Dr. W. H. Avery
Applied Physics Laboratory
8621 Georgia Avenue
Silver Spring, Md. (1 cy)

Dr. Albert Lightbody
Naval Ordnance Laboratory
Plastics Division
White Oak, Silver Spring, Md. (1 cy)

Hercules Powder Company
Allegheny Ballistics Company
Cumberland, Md.
ATTN: Dr. L. G. Benner (1 cy)

Chief, Bureau of Ships
Department of Navy
Washington 25, D. C.
ATTN: Code 344b (2 cys)

Chief, Bureau of Ships
Department of Navy
Washington 25, D. C.
ATTN: Code 660E5 (1 cy)

Chief, Bureau of Ships
Department of Navy
Washington 25, D. C.
ATTN: Code 934 (1 cy)

Chief, Bureau of Ships
Department of Navy
Washington 25, D. C.
ATTN: Code 337L (2 cys)

Chief, Bureau of Ships
Department of Navy
Washington 25, D. C.
ATTN: Code 241 (1 cy)

Director, Material Laboratory
New York Naval Shipyard
Brooklyn 1, N. Y.
ATTN: Code 958 (1 cy)

Chief, Bureau of Aeronautics
Department of Navy
Washington 25, D. C.
ATTN: Code AE-44 (2 cys)

Naval Air Experimental Section
U. S. Naval Base
Philadelphia, Pa.
ATTN: Aeronautical Materials
Laboratory (2 cys)